

Prostate Cancer Detection Using Crawling Wave Sonoelastography

Benjamin Castaneda^{*a,b}, Liwei An^a, Shuang Wu^a, Laurie L. Baxter^c, Jorge L. Yao^c, Jean V. Joseph^d, Kenneth Hoyt^e, John Strang^f, Deborah J. Rubens^f, Kevin J. Parker^a

^aDepartment of Electrical & Computer Eng., University of Rochester, Rochester, NY, USA 14627; ^bGrupo de Formación y Procesamiento de Imágenes Médicas, Sección Electricidad y Electrónica, Departamento de Ingeniería, Pontificia Universidad Católica del Perú, Lima, Perú; ^cDepartment of Pathology & Lab Medicine, University of Rochester Medical Center, Rochester, NY, USA 14642; ^dDepartment of Urology, University of Rochester Medical Center, Rochester, NY, USA 14642; ^eDepartment of Radiology, University of Alabama at Birmingham, Birmingham, AL, USA 35294; ^fDepartment of Imaging Sciences, University of Rochester Medical Center, Rochester, NY, USA 14642

ABSTRACT

Crawling wave (CrW) sonoelastography is an elasticity imaging technique capable of estimating the localized shear wave speed in tissue and, therefore, can provide a quantitative estimation of the Young's modulus for a given vibration frequency. In this paper, this technique is used to detect cancer in excised human prostates and to provide quantitative estimations of the viscoelastic properties of cancerous and normal tissues. Image processing techniques are introduced to compensate for attenuation and reflection artifacts of the CrW images. Preliminary results were obtained with fifteen prostate glands after radical prostatectomy. The glands were vibrated at 100, 120 and 140Hz. At each frequency, three cross-sections of the gland (apex, mid-gland and base) were imaged using CrW Sonoelastography and compared to corresponding histological slices. Results showed good spatial correspondence with histology and an 80% accuracy in cancer detection. In addition, shear velocities for cancerous and normal tissues were estimated as 4.75 ± 0.97 m/s and 3.26 ± 0.87 m/s, respectively.

Keywords: Elasticity imaging, tissue characterization, crawling wave sonoelastography, image processing, prostate cancer detection.

1. INTRODUCTION

Prostate cancer is the most prevalent type of cancer in men, and it is second only to lung cancer in mortality among adult males in the United States. The number of deaths in 2008 was estimated as 28,660 while the new cases diagnosed was calculated as 186,320 [1]. Early and accurate detection is important to reduce mortality and to prevent side effects from local symptoms such as bleeding, urinary tract obstruction and development of metastases. Current prostate cancer diagnosis relies on a combination of digital rectal examination (DRE), screening based on prostate specific antigen levels (PSA) and biopsy guided by transrectal ultrasound (TRUS) imaging. These methods have shown shortcomings in accuracy and specificity and, therefore, new diagnostic tools are required. DRE is limited anatomically to the posterior of the gland and may miss cancers in other regions [2]. Also, PSA levels can be increased not only by cancer but other conditions such as hyperplasia and prostatic inflammation [3]. To further complicate prostate cancer detection, TRUS imaging fails to discriminate isoechoic cancers making random biopsies necessary [4]. However, a high number of biopsies per patient yields a low number of cancers detected with this procedure [5].

DRE is based on the premise that pathological processes produce changes in tissue mechanical properties. Under this rationale, imaging the elastic properties of biological tissues has become an area of active research [6,7,8] with several efforts focused on prostate cancer detection [5,9,10,11,12]. In particular, Crawling wave (CrW) sonoelastography [13] is a recently developed technique capable of estimating the shear wave speed in tissue and, therefore, it can provide a quantitative estimation of the Young's modulus for a given vibration frequency. By taking several measurements at different vibration frequencies, the viscoelastic properties of the tissue can be inferred. This approach was used by Zhang *et al.* [14] to measure the viscoelastic properties of veal liver, thermal-treated veal liver and human prostate *ex vivo*. For all these cases, it was observed that the Young's modulus slightly increased with frequency. Furthermore, the measurements obtained with CrW sonoelastography agreed with the results of a mechanical measurement method based on the Kelvin Voigt fractional derivative model.

*castaned@ece.rochester.edu; phone 1 585 748-3744; fax 1 585 273-4919

In this work, CrW sonoelastography is applied to *ex vivo* human prostate glands to evaluate its performance in cancer detection. Image processing techniques are introduced to compensate for attenuation and reduce artifacts due to poor signal-to-noise ratio (SNR) and possible reflections at boundaries. Furthermore, CrW sonoelastography is used to quantify the viscoelastic properties of normal and cancerous prostate tissue.

2. CRAWLING WAVE SONOELASTOGRAPHY

2.1 Theory

Wu and colleagues [13] proposed the experimental setup described in Figure 1 to image the shear wave interference pattern created by two external sources using sonoelastography [15]. Two mechanical devices are placed opposing each other. The resulting shear waves interfere with each other and are imaged by the transducer sitting on top of the sample. Since sonoelastography only images the particle motion along the ultrasound beam, only the y component of the wave motion is analyzed.

Under the plane wave assumption and considering a homogenous sample, the shear waves introduced by the right and left vibration sources can be described as follows:

$$W_{right} = e^{-\alpha(x+D/2)} e^{-i(k_1(x+D/2)-w_1t)} \quad (1)$$

$$W_{left} = e^{-\alpha(x-D/2)} e^{-i(k_2(x-D/2)-w_2t)} \quad (2)$$

where α is related to the attenuation of the wave in the sample, D is the distance between the sources k_1 and k_2 are the wave numbers and w_1 and w_2 are the frequencies of the vibration sources. The resulting pattern is the superposition of the two waves. For the case in which $w=w_1=w_2$ and $k=k_1=k_2$, the squared signal envelope will result in:

$$|u(x,t)|^2 = (W_{right} + W_{left})(W_{right}^* + W_{left}^*) \quad (3)$$

$$|u(x,t)|^2 = e^{(-\alpha D)} [e^{2\alpha x} + e^{-2\alpha x} + e^{2ikx} + e^{-2ikx}] \quad (4)$$

$$|u(x,t)|^2 = 2e^{(-\alpha D)} [\cosh(2\alpha x) + \cos(2kx)] \quad (5)$$

The interference pattern described in Equation 5 depends on a hyperbolic cosine and a cosine term. In the central region and under weak attenuation, the hyperbolic cosine term can be dropped. Under such consideration, the spatial frequency of the interference patterns becomes $2k$. Thus, the interference fringe spacing is half the intrinsic shear wave wavelength (λ). The shear wave velocity can be estimated as:

$$V_{shear} = f \cdot \lambda \quad (6)$$

where f is controlled and given by the vibration sources and λ is measured from the image. In soft tissue, the relationship between Young's modulus and shear wave velocity can be approximated as:

$$E = 3\rho(V_{shear})^2 \quad (7)$$

where ρ is the mass density and considered to be approximately 1 g/mL.

By introducing a slight offset between the vibration sources ($k_1=k$, $k_2=k+\Delta k$, $w_1=w$, $w_2=w+\Delta w$), Equation 5 is transformed into:

$$|u(x,t)|^2 = 2 \exp(-\alpha D) [\cosh(2\alpha x) + \cos(2kx + \Delta kx + \Delta wt)] \quad (8)$$

The cosine term is now time dependent. Visually, the interference pattern will slowly move towards the source with lower frequency. These moving patterns were termed "Crawling Waves". The advantage of having CrW, as opposed to a static interference pattern, is that they provide more observations to estimate the shear velocity of the sample. Problems due to tissue attenuation and small region of interest (as compared to the shear wave wavelength) can be overcome using CrW. Furthermore, we can use the relationship among frames in a movie to improve the SNR and compensate for attenuation effects as discussed in the next section.

Local estimation of shear velocity allows for the creation of an image representing the elasticity modulus of the sample. This kind of image can be used to establish the size and boundaries of tumors in the prostate and estimate the elasticity modulus of normal and cancerous tissue. Hoyt *et al.* [16] proposed a two-dimensional real-time estimator based on

autocorrelation methods. One of the main advantages of this method is its computational simplicity, comparable to current color flow processing available in commercial US scanners.

2.2 Enhancement of CrW images

The accuracy of the estimation of the shear velocity spatial distribution depends on the quality of the crawling waves. This section introduces a pre-processing scheme to improve the SNR of the CrW images by taking into account the time relationship among the frames of a CrW movie (cine loop) while it is imaging the same spatial location. An additional advantage of this processing is the generation of a quality metric which can be used to discriminate the shear velocity information accordingly. Figure 2 summarizes the proposed approach. A CrW movie is taken at a single position in the tissue. Each frame of the movie is processed using a median filter to reduce the noise. Due to the nature of CrW imaging, the median filter uses a support kernel which is larger than wider (*i.e.* [11x3]). Subsequently, the images are improved by 3 processes: Horizontal and vertical motion filtering, slow time filtering and a phase multiplication.

First, a horizontal motion filter [17] is applied to improve SNR and reduce potential reflection artifacts. A horizontal line from the CrW movie (blue line in Figure 3a) is followed in time to form a 2D image which would ideally look like Figure 3c. The 2D Fourier transform of such an image would have its energy concentrated in two peaks (sinusoidal in time and space) of known frequencies since the speed of the CrW and the Doppler frame rate are controlled. A band-pass filter (Figure 3d) is applied to reduce noise and artifacts. This operation is repeated for all the lines in the CrW movie. Similarly, a vertical motion filter is applied. In this case, a vertical line is followed in time to form an image, and a low-pass filter is employed since most of the energy is concentrated in the time axis.

Subsequently a slow time filter is applied to compensate for attenuation and to improve the SNR. This filter processes the signal obtained from a single spatial position (*i.e.* pixel) in time. Since the CrW are governed by Equation 8, the signal in each pixel should vary following a sinusoidal pattern of frequency Δw . The slow time signals are then fit into a sinusoidal model:

$$Y = A \cos(\Delta w X + \theta) + D \quad (9)$$

where Y is the value of the slow time signal, and X is the independent variable which corresponds to the frame number. A, θ , and D are the parameters of the model to be estimated and correspond to the amplitude, phase and offset of the signal, respectively. Two images are obtained as a result of the slow time processing: A phase image and an r^2 -value image. The latter represents the goodness of fit in the optimization process for each of the pixels in the CrW movie and it is employed as a quality index. Pixels with r^2 lower than 0.6 are not considered for further processing.

From the phase image, a filtered version of the CrW movie can be reconstructed. In this filtered version, the CrW have normalized amplitude and noise effects have been considerably reduced. In order to improve the estimation of shear velocity using the autocorrelation approach [16], the phase image is multiplied by a factor of four. As a consequence, the final processed CrW movie has four times the spatial frequency than its original version.

2.3 Pseudo-sonoelastographic images

Sonoelastography is a tissue elasticity imaging technique that estimates the amplitude response of tissues under harmonic mechanical excitation using ultrasonic Doppler techniques [15]. Due to the relationship between particle vibrational response and received Doppler spectral variance [18], the amplitude of low frequency shear waves propagating in tissue can be visualized in real-time using sonoelastography to detect regions of abnormal stiffness [19]. Clinical research in sonoelastography has focused primarily on prostate cancer detection. An initial comparison between sonoelastographic images and corresponding histological slides with promising results was reported by Rubens *et al.* in 1995 [20]. An experimental setup for three-dimensional sonoelastography was built by Taylor and colleagues. Their results indicated that sonoelastography had the capability to detect lesions over 1cc [5]. More recently, initial results of undergoing studies have been presented, including an extension to *in vivo* imaging [12]. It is possible to reconstruct an image equivalent to the sonoelastographic image from a CrW movie. This pseudo-sonoelastographic image is created by taking the maximum of the same signal used in slow time filtering: The maximum of the values each pixel takes over time. Therefore it is possible to compare results from CrW and (pseudo) sonoelastographic images.

3. MATERIALS AND METHODS

3.1 Simulations

A CrW movie on a homogeneous media was simulated to test the performance of the motion filtering, slow time filtering and phase multiplication stages under the presence of noise and reflection artifacts. The estimation of the shear velocity using the local autocorrelation method was compared with: no filtering, only slow-time filtering, and both motion and slow-time filtering. In addition, the changes in the estimation were compared with and without phase multiplication.

3.2 Experiments

Fifteen prostatic glands were obtained after radical prostatectomy and embedded in a 10.5% gelatin mold. Two pistons (Model 2706, Brüel & Kjaer, Naerum, Denmark) were fitted with surface-abraded extensions and located at each side of the mold to create shear vibration (see Figure 1). The ultrasound transducer (M12L, General Electric Healthcare, Milwaukee, WI, USA) was positioned on top of the gelatin mold and equidistant from the vibration sources. Each gland was imaged at three locations: AB1, AB2, and AB3. These locations were chosen to capture images close to the apex (AB1), at middle gland (AB2), and close to the base (AB3). Three movies of CrW images, each one with a different vibration frequency (100, 120 and 140 Hz), were acquired at each of the locations. In all cases the frequency offset between the vibration sources was set to 0.25 Hz. The site for the three cross-sections was marked and the corresponding histological slices were obtained. An expert pathologist outlined the cancerous regions in the histological slices. This information was considered as ground truth.

The CrW images were pre-processed following the enhancement methods described in the previous section. Subsequently, a two-dimensional shear wave velocity estimator [16], with a kernel of 20 by 20, was used to obtain an estimate of the shear velocity of the tissue for each of the vibration frequencies. Using the quality metric obtained from slow time filtering, the best two estimations were averaged into a final image representing the shear velocity. This image and its corresponding histological slice were divided in quadrants and compared to evaluate the performance of the CrW technique in cancer detection. To quantify the viscoelastic characteristics of cancerous and normal tissue, the elasticity modulus of true positive and true negative areas were measured. A region was marked as cancer on the CrW elasticity image if it had a shear velocity that was greater or equal to 1.25 times that of the surrounding prostate tissue. A seed growing algorithm was used to segment these regions of elevated shear velocity [21]. In addition, pseudo-sonoelastographic images were reconstructed and compared to histology.

4. RESULTS

4.1 Simulations

Figure 4 illustrates the results from the shear velocity estimator when applied (a) directly to the simulated CrW movie, (b) after slow-time filtering, and (c) after motion and slow time filtering. The CrW movie was simulating a homogenous region with shear velocity = 3 m/s. In the first case (a), the autocorrelation method failed to estimate the correct shear velocity in the presence of noise. In the second case (b), slow time filtering is able to improve the SNR of the CrW movie, but it is still susceptible to the presence of reflections which produce a ripple artifact in the estimation. The combination of motion and slow-time filtering (c) compensates for the noise and the reflection problems providing a more constant result.

Figure 5 presents the results from the shear velocity estimator (a) without and (b) with a phase multiplication of four applied to the simulated CrW movie (shear velocity = 3 m/s). Estimations with the autocorrelation method were evaluated using several kernel sizes. The results after phase multiplication showed a more uniform estimation even when a smaller kernel size was used.

4.2 Experiments

Representative cases from two *ex vivo* prostate glands, one without cancer and the other with, are presented in Figure 6 and 7. Figure 6 shows CrW images with (a) and without phase multiplication (b). The corresponding shear velocity estimation (c) does not indicate the presence of any stiff region. Histology revealed that this particular cross-section did not have cancer. In Figure 7, the corresponding B-mode (a), shear speed (b) and histological (c) images of a cross-section close to the apex (AB1) of a human prostate gland are shown. The shear speed image shows an area with elevated shear speed on the left side of the cross-section which corresponds to a cancerous region in the histological image.

Table 1 summarizes the performances of CrW sonoelastography and pseudo-sonoelastography for prostate cancer detection in terms of accuracy, sensitivity and specificity. Three cross-sections from each of the fifteen prostate glands were analyzed. Out the forty-five samples, four were discarded due to poor SNR. These cross-sections were closed to the base of the gland (AB3) and showed a very low quality metric (<0.6). CrW sonoelastography outperforms pseudo-sonoelastography. The shear velocity for all included cancerous and normal tissues was estimated as 4.75 ± 0.97 m/s and 3.26 ± 0.87 m/s, respectively.

In order to understand the viscoelastic effect in the range of frequencies used (100-140Hz), five cross-sections that contained no detectable cancer were analyzed. Results from this quantitative analysis are shown in Table 2. The increment in shear velocity with frequency is indicative of a viscoelastic effect.

5. DISCUSSION

This work evaluates the performance of Crawling Wave Sonoelastography for prostate cancer detection *ex vivo*. Additionally, the quantitative nature of CrW Sonoelastography allows estimating the viscoelastic properties of the analyzed glands. Pseudo-sonoelastographic images are reconstructed from CrW movies in order to compare both techniques. Performance of pseudo-sonoelastography in cancer detection is similar to previously reported results [5,12,20]. In general, CrW sonoelastography outperforms pseudo-sonoelastography; however, a combination of both modalities might provide a better performance in cancer detection. In particular, it was observed that a high elastic contrast could create a region with a very low SNR. Although this condition produced high contrast in pseudo-sonoelastographic images, it damages the slow time filtering as well as the estimation processes in CrW sonoelastography.

A protocol to analyze the properties of prostate glands *ex vivo* was developed. A critical part of this process is to mark the cross-section of the gland which is imaged in order to obtain the corresponding histological image (ground truth). Currently, the imaging plane is marked using surgical needles. Even though, the marking is done with extreme care, the imaging and histological planes may not match precisely. Errors in the insertion of the needle as well as deviations when cutting prostate gland may introduce differences which may be carried into the evaluation of the performance.

An initial analysis of the viscoelastic properties of normal prostate tissue showed that the variation in elasticity is small in the range of frequencies utilized. Therefore, averaging the results of two different frequencies is not only valid but it should improve the final estimation since it is based on two independent results.

There is a compromise in the selection of the kernel size for the autocorrelation estimator. Having a larger kernel provides estimations less susceptible to the starting phase of the signal but it reduces the field of view and smoothes the results. Phase multiplication, as shown in Figure 5b, permits estimation comparable to the findings without phase multiplication but with smaller kernel sizes.

Estimated shear velocity values for normal and cancerous tissue are slightly elevated but in the same order of magnitude when compared to previous findings based on mechanical testing using a Kelvin-Voight Fractional Derivative model [22]. However, it is important to note that values from mechanical testing were from samples containing both cancerous and normal tissue. Therefore, it is expected that only cancerous tissue will have higher values. Results indicate that it is possible to differentiate pathological from normal tissue using CrW.

6. CONCLUSION

In this paper, Crawling Wave (CrW) Sonoelastography is used to detect cancer in excised human prostates and provide quantitative estimations of the viscoelastic properties of human cancerous and normal tissues. Results showed good spatial correspondence with histology. Additionally, the estimated shear velocities of cancerous and normal tissue are 4.75 ± 0.97 m/s and 3.26 ± 0.87 m/s, respectively. These results are in agreement with previous reports on the elasticity of cancerous and normal human prostate tissue and suggest that CrW Sonoelastography could be used to improve prostate cancer detection.

ACKNOWLEDGEMENTS

The authors would like to thank GE Ultrasound for their support and Dr. Jay Hah for his comments on the final manuscript. This work was funded by NIH Grant 5R01AG016317-07.

REFERENCES

- [1] American Cancer Society - Cancer Facts and Figures 2008, American Cancer Society (2008).
- [2] Reissigl, A., Pointner, J., Strasser, H., Ennemoser, O., Klocker H., and Bartsch, G., "Frequency and clinical significance of transition zone cancer in prostate cancer screening," *Prostate*, 30, 130–135 (1997).
- [3] Benson, M.C. and Olsson, C.A., "Prostate specific antigen and prostate specific antigen density: Roles in patient evaluation and management," *Cancer*, 74, 1667-1673 (1994).
- [4] Ellis, W.J. and Brawer, M.K., "The significance of isoechoic prostatic carcinoma," *J. Urol.*, 152, 2304–2307 (1994).
- [5] Taylor, L.S., Rubens, D.J., Porter, B.C., Wu, Z., Baggs, R.B., di Sant'Agnese, P.A., et al., "Prostate cancer: Sonoelastography for in vitro detection", *Radiology*, 237, 981-985 (2005).
- [6] Gao, L., Parker, K.J., Lerner, R.M., and Levinson, S.F., "Imaging of the elastic properties of tissue - A review," *Ultrasound Med. Biol.*, 22, 959-977 (1996).
- [7] Ophir, J., Alam, S.K., Garra, B., Kallel, F., Konofagou, E., Krouskop, T., and Varghese, T., "Elastography: Ultrasonic estimation and imaging of the elastic properties of tissues," *Proc. Instn. Mech. Engrs.*, 213, 203-233 (1999).
- [8] Greenleaf, J., Fatemi, M., and Insana, M., "Selected methods for imaging elastic properties of biological tissues," *Annu. Rev. Biomed. Eng.*, 5, 57-78 (2003).
- [9] Lorenz, A., Sommerfeld, H., Garcia-Schurmann, M., Philippou, S., Senge, T., and Ermert, H., "A new system for the acquisition of ultrasonic multicompression strain images of the human prostate in vivo," *IEEE Trans. Ultrason. Ferroelec. Freq. Contr.*, 46, 1147-1153 (1999).
- [10] Pesavento, A., and Lorenz, A., "Real time strain imaging and in vivo applications in prostate cancer," *Proc. IEEE Ultrason. Symp.*, 2, 1647-1652 (2001).
- [11] Souchon, R., Rouviere, O., Gelet, A., Detti, V., Srinivasan, S., Ophir, J., and Chapelon, J.Y., "Visualisation of HIFU lesions using elastography of the human prostate in vivo: Preliminary results," *Ultrasound Med. Biol.*, 29, 1007-1015 (2003).
- [12] Hoyt, K., Castaneda, B., Zhang, M., Nigwekar, P., di Sant'Agnese, P.A., Joseph, J.V., Strang, J., Rubens, D.J., Parker, K.J., "Tissue elasticity properties as biomarkers for cancer in prostate," *Cancer Biomarkers*, 4, 213-225 (2008).
- [13] Wu, Z., Hoyt, K., Rubens, D.J., Parker, K.J., "Sonoelastographic imaging of interference patterns for estimation of shear velocity distribution in biomaterials," *J. Acoust. Soc. Am.*, 120, 535-545 (2006).
- [14] Zhang, M., Castaneda, B., Wu, Z., Nigwekar, P., Joseph, J.V., Rubens D.J., Parker K.J., "Congruence of imaging estimator and mechanical measurements of viscoelastic properties of soft tissues," *Journal of Ultrasound in Medicine and Biology*, 33, 1617-1631 (2007).
- [15] Lerner, R.M., Parker, K.J., Holen, J., Gramiak, R., and Waag, R.C., "Sonoelasticity: Medical elasticity images derived from ultrasound signals in mechanically vibrated targets," *Acoust. Imaging*, 16, 317-327 (1988).
- [16] Hoyt, K., Castaneda, B., Parker, K.J., "Two dimensional sonoelastographic shear velocity imaging", *Journal of Ultrasound in Medicine and Biology*, 34, 276-288 (2008).
- [17] Thomas, A., McLaughlin, J.R., Lin, K., "Two dimensional shear wave speed and crawling wave speed recoveries from in vitro prostate data," *Proceedings of the Seventh International Conference on the Ultrasonic Measurement and Imaging of Tissue Elasticity*, 101 (2008).
- [18] Huang, S.R., Lerner, R.M. and Parker, K.J., "On estimating the amplitude of harmonic vibration from the Doppler spectrum of reflected signals," *J. Acoust. Soc. Am.*, 88, 310-317 (1990).
- [19] Parker, K.J., Fu, D., Gracewski, S.M., Yeung, F., and Levinson, S.F., "Vibration sonoelastography and the detectability of lesions", *Ultrasound Med. Biol.*, 24, 1937-1947 (1998).
- [20] Rubens, D.J., Hadley, M.A., Alam, S.K., Gao, L., Mayer, R.D., and Parker, K.J., "Sonoelasticity imaging of prostate cancer: in vitro results," *Radiology*, 195, 379-383 (1995)

- [21] Castaneda, B., Tamez-Pena, J.G., Zhang, M., Hoyt, K., Bylund, K., Christensen, J., Saad, W., Strang, J., Rubens, D.J., and Parker, K.J., "Measurement of thermally-ablated lesions in sonoelastographic images using level set methods," *Proceedings of SPIE*, 6920, 692018-1 – 692018-8 (2008).
- [22] Zhang, M., Nigwekar, P., Castaneda, B., Hoyt, K., Joseph, J.V., di Sant'agnese, A., Messing, E.M., Strang, J.G., Rubens, D.J., and Parker, K.J., "Quantitative characterization of viscoelastic properties of human prostate correlated with histology," *Journal of Ultrasound in Medicine*, 34, 1033-1042 (2008).

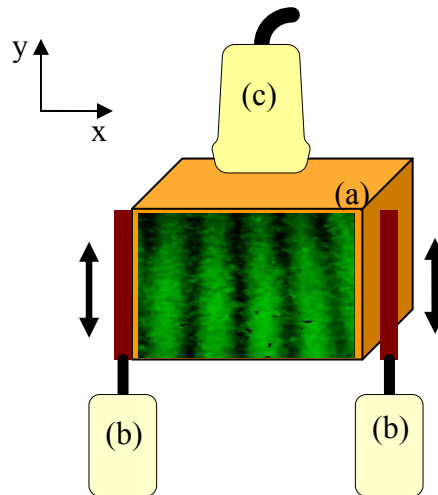


Figure 1. Schematic of the experimental setup. The prostate gland embedded in a gelatin mold (a) is located between two shear vibration sources (b). The ultrasound transducer is positioned on top to acquire the crawling wave images (c).

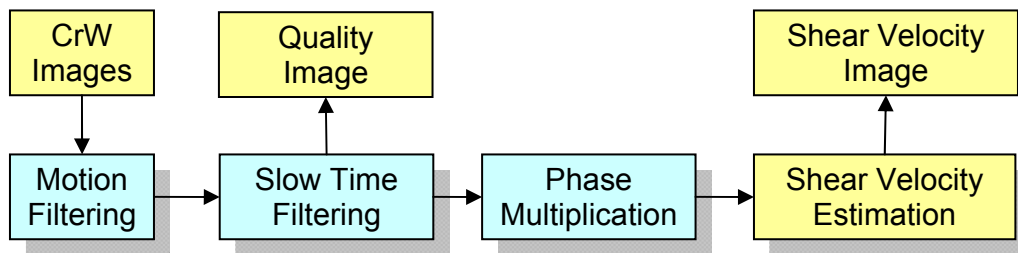


Figure 2. Proposed scheme to enhance the crawling wave images.

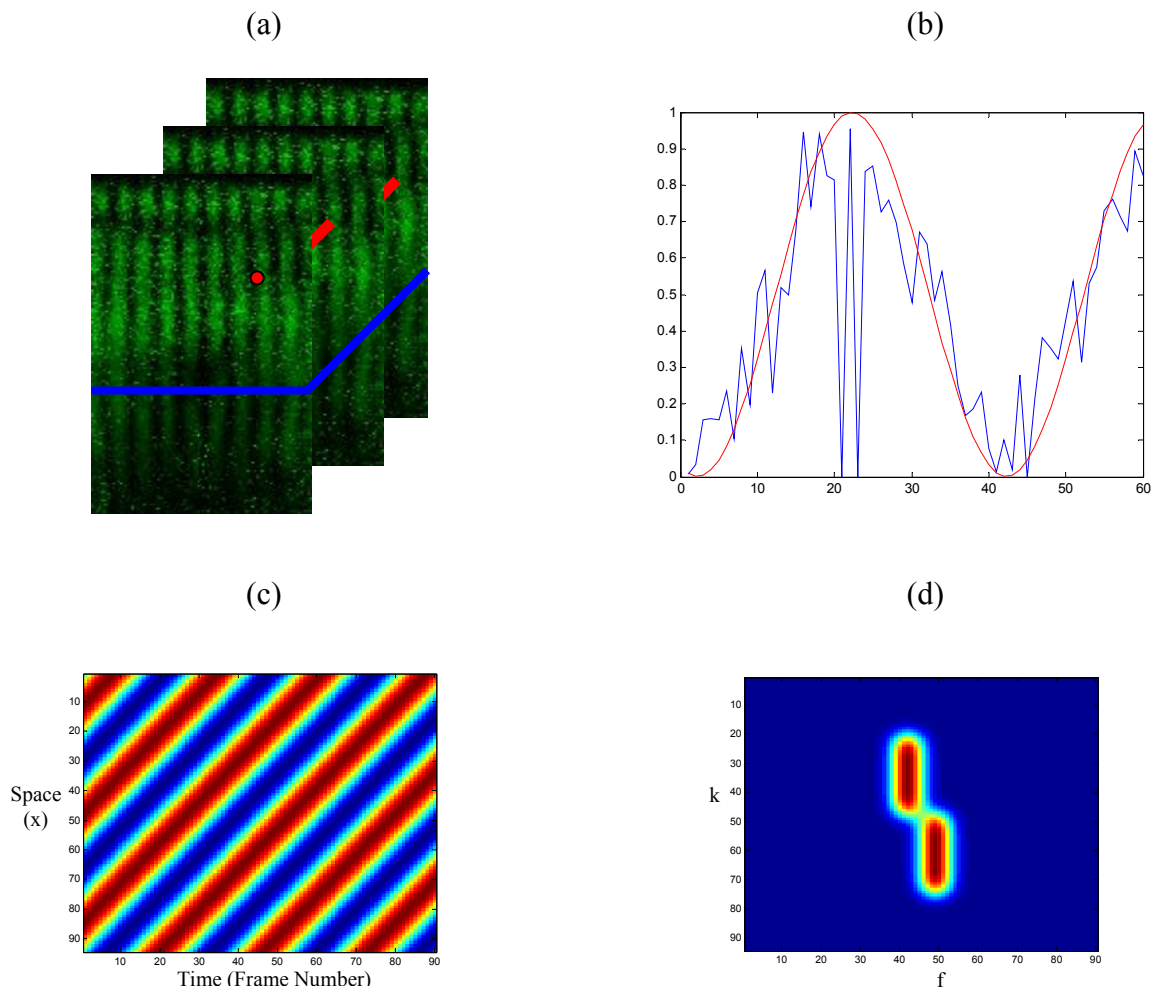


Fig. 3. Slow-Time and Motion Filters. The slow time signal at each pixel of the crawling wave movie (red line in a) is replaced with its sinusoidal version. The original signal and its sinusoidal correction are plotted in (b) in blue and red colors, respectively. (c) shows an image representing the evolution of a single line in the CrW movie (blue line in a), and (d) presents a band pass filter used for motion filtering.

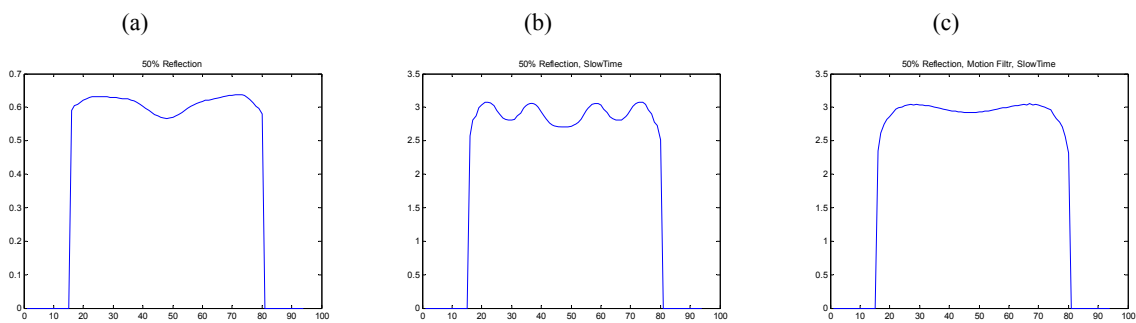


Figure 4. Results from the shear velocity estimator applied directly to the simulated CrW movie (a), applied after slow time filtering (b), and applied after motion and slow time filtering. The CrW simulated a homogenous region with shear velocity = 3 m/s.

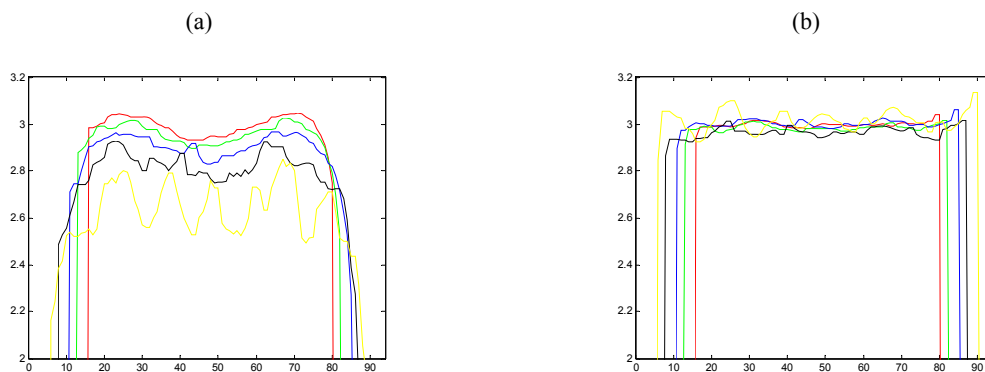


Figure 5. Results from the shear velocity estimator (a) without and (b) with phase multiplication of four. The CrW were simulated in a homogenous region with shear velocity = 3 m/s. The estimations were performed with kernel sizes of 30x30 (red), 25x25 (green), 20x20 (blue), 15x15 (black) and 10x10 (yellow). Estimations after phase multiplication show a more uniform behavior.

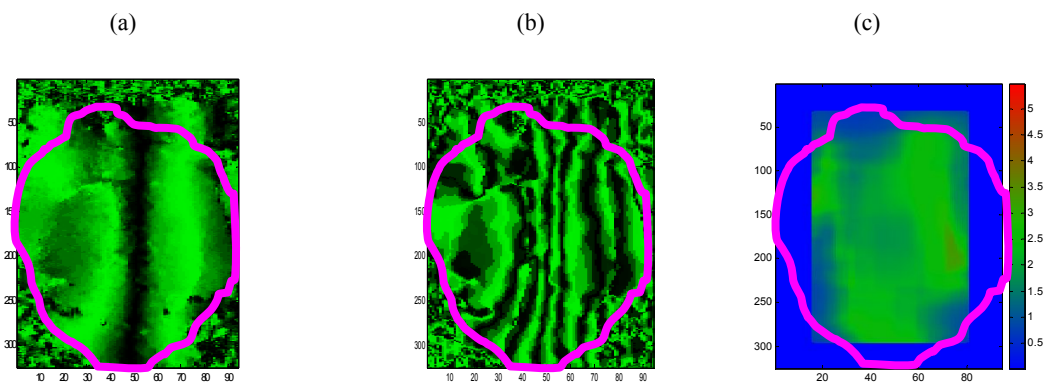


Figure 6. CrW image without (a) and with (b) phase multiplication; and its corresponding shear velocity image (c). Histology revealed that this cross-section did not have cancer. The boundary of the prostate gland is shown in pink.

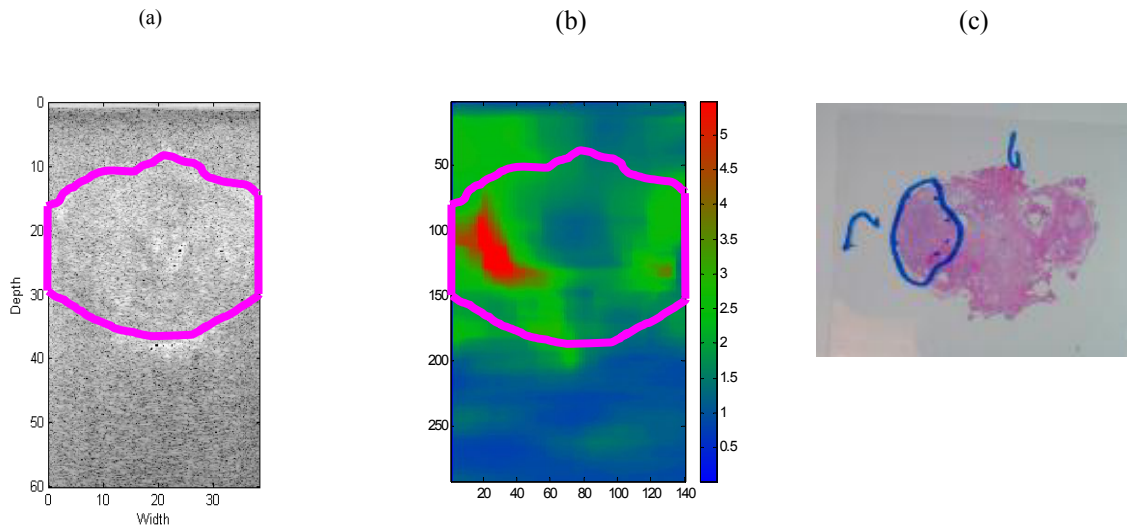


Figure 7. Corresponding B-mode (a), shear speed (b) and histological (c) images of a cross-section close to the apex of a human prostate gland. The shear speed image shows a region with elevated shear speed on the left side of the cross-section which corresponds to a cancerous region in the histological image.

Table 1. Performance in prostate cancer detection (N=41 cross-sections x 4 quadrants).

	Accuracy (%)	Sensitivity (%)	Specificity (%)
CrW Sonoelastography	80.4	67.3	86.2
Pseudo Sonoelastography	67.9	60.8	70.9

Table 2. Estimated shear wave speeds for normal prostate tissue (N=5 cross-sections with no cancer).

	100Hz (m/s)	120Hz (m/s)	140Hz (m/s)
Normal Tissue	2.9±0.4	3.1±0.4	3.3±0.5